

# The dark atoms of dark matter

Maxim Yu. Khlopov\*, Andrey G. Mayorov<sup>†</sup> and Evgeny Yu. Soldatov\*\*

\*Centre for Cosmoparticle Physics "Cosmion" 115409 Moscow, Russia;  
National Research Nuclear University "Moscow Engineering Physics Institute", 115409 Moscow, Russia  
APC laboratory 10, rue Alice Domon et Léonie Duquet  
75205 Paris Cedex 13, France  
khlopov@apc.univ-paris7.fr

<sup>†</sup>National Research Nuclear University (Moscow Engineering Physics Institute)  
115409 Moscow, Russia  
mayorov.a.g@gmail.com

\*\*National Research Nuclear University (Moscow Engineering Physics Institute)  
115409 Moscow, Russia  
Evgeny.Soldatov@cern.ch

**Abstract.** The nonbaryonic dark matter of the Universe is assumed to consist of new stable particles. A specific case is possible, when new stable particles bear ordinary electric charge and bind in heavy "atoms" by ordinary Coulomb interaction. Such possibility is severely restricted by the constraints on anomalous isotopes of light elements that form positively charged heavy species with ordinary electrons. The trouble is avoided, if stable particles  $X^{--}$  with charge -2 are in excess over their antiparticles (with charge +2) and there are no stable particles with charges +1 and -1. Then primordial helium, formed in Big Bang Nucleosynthesis, captures all  $X^{--}$  in neutral "atoms" of O-helium (OHe), thus creating a specific Warmer than Cold nuclear-interacting composite dark matter. In the Galaxy, destruction of OHe and acceleration of free  $X^{--}$  can result in anomalous component of cosmic rays. Collisions of OHe atoms in the central part of Galaxy results in their excitation with successive emission of electron-positron pairs, what can explain excessive radiation of positron annihilation line, observed by INTEGRAL. Slowed down in the terrestrial matter, OHe is elusive for direct methods of underground dark matter detection based on the search for effects of nuclear recoil in WIMP-nucleus collisions. However OHe-nucleus interaction leads to their binding and in OHe-Na system the energy of such level can be in the interval of energy 2-4 keV. The concentration of OHe in the matter of underground detectors is rapidly adjusted to the incoming flux of cosmic O-helium. Therefore the rate of energy release in radiative capture of Na by OHe should experience annual modulations. It explains the results of DAMA/NaI and DAMA/LIBRA experiments. The existence of low energy bound state in OHe-Na system follows from the solution of Schrodinger equation for relative motion of nucleus and OHe in a spherically symmetrical potential, formed by the Yukawa tail of nuclear scalar isoscalar attraction potential, acting on He beyond the nucleus, and its Coulomb repulsion at distances from nuclear surface, smaller than the size of OHe. Within the uncertainties of nuclear physics parameters the values of coupling strength and mass of sigma meson, mediating scalar isoscalar nuclear potential, are found, at which the sodium nuclei have a few keV binding energy with OHe. Transitions to more energetic levels of Na+OHe system imply tunneling through Coulomb barrier that leads to suppression of annual modulation of events with MeV-tens MeV energy release in the correspondence with the results of DAMA experiments. The puzzles of direct dark matter searches appear in this solution as a reflection of nontrivial nuclear physics of OHe.

**Keywords:** elementary particles, nuclear reactions, nucleosynthesis, abundances, dark matter, early universe, large-scale structure of universe

**PACS:** 12.60.Cn,98.90.+s,12.60.Nz,14.60.Hi,26.35.+c,36.90.+f,03.65.Ge

## INTRODUCTION

According to the modern cosmology, the dark matter, corresponding to 25% of the total cosmological density, is nonbaryonic and consists of new stable particles. One can formulate the set of conditions under which new particles can be considered as candidates to dark matter (see e.g. [1, 2, 3] for review and reference): they should be stable, saturate the measured dark matter density and decouple from plasma and radiation at least before the beginning of matter dominated stage. The easiest way to satisfy these conditions is to involve neutral elementary weakly interacting particles. However it is not the only particle physics solution for the dark matter problem and more evolved models of self-interacting dark matter are possible. In particular, new stable particles may possess new U(1) gauge charges and bind by Coulomb-like forces in composite dark matter species. Such dark atoms would look nonluminous, since they radiate invisible light of U(1) photons. In the studies of new particles Primordial Black holes can play the role of

important theoretical tool (see [4] for review and references), which in particular can provide constraints on particles with hidden gauge charges [5].

Here we consider composite dark matter scenarios, in which new stable particles have ordinary electric charge, but escape experimental discovery, because they are hidden in atom-like states maintaining dark matter of the modern Universe. The main problem for these scenarios is to suppress the abundance of positively charged species bound with ordinary electrons, which behave as anomalous isotopes of hydrogen or helium. This problem is unresolvable, if the model predicts together with positively charged particles stable particles  $E^-$  with charge -1, as it is the case for teraelectrons [6, 7]. As soon as primordial helium is formed in the Standard Big Bang Nucleosynthesis (SBBN) it captures all the free  $E^-$  in positively charged  $(HeE)^+$  ion, preventing any further suppression of positively charged species. Therefore, in order to avoid anomalous isotopes overproduction, stable particles with charge -1 should be absent, so that stable negatively charged particles should have charge -2 only.

Elementary particle frames for heavy stable -2 charged species are provided by: (a) stable "antibaryons"  $\bar{U}\bar{U}\bar{U}$  formed by anti- $U$  quark of fourth generation [8, 9, 10, 11] (b) AC-leptons [11, 12, 13], predicted in the extension [12] of standard model, based on the approach of almost-commutative geometry [14]. (c) Technileptons and anti-technibaryons [15] in the framework of walking technicolor models (WTC) [16]. (d) Finally, stable charged clusters  $\bar{u}_5\bar{u}_5\bar{u}_5$  of (anti)quarks  $\bar{u}_5$  of 5th family can follow from the approach, unifying spins and charges [17]. Since all these models also predict corresponding +2 charge antiparticles, cosmological scenario should provide mechanism of their suppression, what can naturally take place in the asymmetric case, corresponding to excess of -2 charge species,  $X^{--}$ . Then their positively charged antiparticles can effectively annihilate in the early Universe.

In all the models, in which new stable species belong to non-trivial representations of electroweak SU(2) group sphaleron transitions at high temperatures provide the relationship between baryon asymmetry and excess of -2 charge stable species [15, 18, 19, 20].

After it is formed in the Standard Big Bang Nucleosynthesis (SBBN),  ${}^4He$  screens the  $X^{--}$  charged particles in composite  $({}^4He^{++}X^{--})$  O-helium "atoms" [9]. For different models of  $X^{--}$  these "atoms" are also called ANO-helium [10, 11], Ole-helium [11, 13] or techni-O-helium [15]. We'll call them all O-helium (OHe) in our further discussion, which follows the guidelines of [19, 20, 21].

In all these forms of O-helium,  $X^{--}$  behaves either as lepton or as specific "heavy quark cluster" with strongly suppressed hadronic interaction. Therefore O-helium interaction with matter is determined by nuclear interaction of  $He$ . These neutral primordial nuclear interacting objects contribute to the modern dark matter density and play the role of a nontrivial form of strongly interacting dark matter [22, 23, 24].

The active influence of this type of dark matter on nuclear transformations needs special studies and development of OHe nuclear physics. It is especially important for quantitative estimation of role of OHe in Big Bang Nucleosynthesis and in stellar evolution. This work is under way and its first results support the qualitative picture of OHe cosmological evolution described in [9, 13, 15, 19, 25].

Here after a brief review of main features of OHe Universe we concentrate on its effects in underground detectors. We qualitatively confirm the earlier guess [9, 18, 19, 20, 21, 26] that the positive results of dark matter searches in DAMA/NaI (see for review [27]) and DAMA/LIBRA [28] experiments can be explained by effects of O-helium interaction with the matter of underground detectors.

## SOME FEATURES OF O-HELIUM UNIVERSE

Following [9, 10, 11, 15, 19, 20, 21] consider charge asymmetric case, when excess of  $X^{--}$  provides effective suppression of positively charged species.

In the period  $100\text{ s} \leq t \leq 300\text{ s}$  at  $100\text{ keV} \geq T \geq T_o = I_o/27 \approx 60\text{ keV}$ ,  ${}^4He$  has already been formed in the SBBN and virtually all free  $X^{--}$  are trapped by  ${}^4He$  in O-helium "atoms"  $({}^4He^{++}X^{--})$ . Here the O-helium ionization potential is<sup>1</sup>

$$I_o = Z_x^2 Z_{He}^2 \alpha^2 m_{He} / 2 \approx 1.6\text{ MeV}, \quad (1)$$

where  $\alpha$  is the fine structure constant,  $Z_{He} = 2$  and  $Z_x = 2$  stands for the absolute value of electric charge of  $X^{--}$ . The size of these "atoms" is [9, 13]

$$R_o \sim 1 / (Z_x Z_{He} \alpha m_{He}) \approx 2 \cdot 10^{-13}\text{ cm} \quad (2)$$

---

<sup>1</sup> The account for charge distribution in  $He$  nucleus leads to smaller value  $I_o \approx 1.3\text{ MeV}$  [29].

Here and further, if not specified otherwise, we use the system of units  $\hbar = c = k = 1$ .

O-helium, being an  $\alpha$ -particle with screened electric charge, can catalyze nuclear transformations, which can influence primordial light element abundance and cause primordial heavy element formation. These effects need a special detailed and complicated study. The arguments of [9, 13, 15, 19, 20] indicate that this model does not lead to immediate contradictions with the observational data. The conclusions that follow from our first steps in the approach to OHe nuclear physics seem to support these arguments.

Due to nuclear interactions of its helium constituent with nuclei in the cosmic plasma, the O-helium gas is in thermal equilibrium with plasma and radiation on the Radiation Dominance (RD) stage, while the energy and momentum transfer from plasma is effective. The radiation pressure acting on the plasma is then transferred to density fluctuations of the O-helium gas and transforms them in acoustic waves at scales up to the size of the horizon.

At temperature  $T < T_{od} \approx 200S_3^{2/3}$  eV the energy and momentum transfer from baryons to O-helium is not effective [9, 15] because

$$n_B \langle \sigma v \rangle (m_p/m_o)t < 1,$$

where  $m_o$  is the mass of the *OHe* atom and  $S_3 = m_o/(1 \text{ TeV})$ . Here

$$\sigma \approx \sigma_o \sim \pi R_o^2 \approx 10^{-25} \text{ cm}^2, \quad (3)$$

and  $v = \sqrt{2T/m_p}$  is the baryon thermal velocity. Then O-helium gas decouples from plasma. It starts to dominate in the Universe after  $t \sim 10^{12}$  s at  $T \leq T_{RM} \approx 1$  eV and O-helium "atoms" play the main dynamical role in the development of gravitational instability, triggering the large scale structure formation. The composite nature of O-helium determines the specifics of the corresponding dark matter scenario.

At  $T > T_{RM}$  the total mass of the *OHe* gas with density  $\rho_d = (T_{RM}/T)\rho_{tot}$  is equal to

$$M = \frac{4\pi}{3} \rho_d t^3 = \frac{4\pi}{3} \frac{T_{RM}}{T} m_{Pl} \left(\frac{m_{Pl}}{T}\right)^2$$

within the cosmological horizon  $l_h = t$ . In the period of decoupling  $T = T_{od}$ , this mass depends strongly on the O-helium mass  $S_3$  and is given by [15]

$$M_{od} = \frac{T_{RM}}{T_{od}} m_{Pl} \left(\frac{m_{Pl}}{T_{od}}\right)^2 \approx 2 \cdot 10^{44} S_3^{-2} \text{ g} = 10^{11} S_3^{-2} M_\odot, \quad (4)$$

where  $M_\odot$  is the solar mass. O-helium is formed only at  $T_o$  and its total mass within the cosmological horizon in the period of its creation is  $M_o = M_{od}(T_{od}/T_o)^3 = 10^{37}$  g.

On the RD stage before decoupling, the Jeans length  $\lambda_J$  of the *OHe* gas was restricted from below by the propagation of sound waves in plasma with a relativistic equation of state  $p = \varepsilon/3$ , being of the order of the cosmological horizon and equal to  $\lambda_J = l_h/\sqrt{3} = t/\sqrt{3}$ . After decoupling at  $T = T_{od}$ , it falls down to  $\lambda_J \sim v_o t$ , where  $v_o = \sqrt{2T_{od}/m_o}$ . Though after decoupling the Jeans mass in the *OHe* gas correspondingly falls down

$$M_J \sim v_o^3 M_{od} \sim 3 \cdot 10^{-14} M_{od},$$

one should expect a strong suppression of fluctuations on scales  $M < M_o$ , as well as adiabatic damping of sound waves in the RD plasma for scales  $M_o < M < M_{od}$ . It can provide some suppression of small scale structure in the considered model for all reasonable masses of O-helium. The significance of this suppression and its effect on the structure formation needs a special study in detailed numerical simulations. In any case, it can not be as strong as the free streaming suppression in ordinary Warm Dark Matter (WDM) scenarios, but one can expect that qualitatively we deal with Warmer Than Cold Dark Matter model.

Being decoupled from baryonic matter, the *OHe* gas does not follow the formation of baryonic astrophysical objects (stars, planets, molecular clouds...) and forms dark matter halos of galaxies. It can be easily seen that O-helium gas is collisionless for its number density, saturating galactic dark matter. Taking the average density of baryonic matter one can also find that the Galaxy as a whole is transparent for O-helium in spite of its nuclear interaction. Only individual baryonic objects like stars and planets are opaque for it.

## SIGNATURES OF O-HELIUM DARK MATTER IN THE GALAXY

The composite nature of O-helium dark matter results in a number of observable effects, which we briefly discuss following [19].

### Anomalous component of cosmic rays

O-helium atoms can be destroyed in astrophysical processes, giving rise to acceleration of free  $X^{--}$  in the Galaxy. O-helium can be ionized due to nuclear interaction with cosmic rays [9, 21]. Estimations [9, 30] show that for the number density of cosmic rays  $n_{CR} = 10^{-9} \text{cm}^{-3}$  during the age of Galaxy a fraction of about  $10^{-6}$  of total amount of OHe is disrupted irreversibly, since the inverse effect of recombination of free  $X^{--}$  is negligible. Near the Solar system it leads to concentration of free  $X^{--}$   $n_X = 3 \cdot 10^{-10} S_3^{-1} \text{cm}^{-3}$ . After OHe destruction free  $X^{--}$  have momentum of order  $p_X \cong \sqrt{2 \cdot M_X \cdot I_o} \cong 2 \text{GeV} S_3^{1/2}$  and velocity  $v/c \cong 2 \cdot 10^{-3} S_3^{-1/2}$  and due to effect of Solar modulation these particles initially can hardly reach Earth [18, 30]. Their acceleration by Fermi mechanism or by the collective acceleration forms power spectrum of  $X^{--}$  component at the level of  $X/p \sim n_X/n_g = 3 \cdot 10^{-10} S_3^{-1}$ , where  $n_g \sim 1 \text{cm}^{-3}$  is the density of baryonic matter gas.

At the stage of red supergiant stars have the size  $\sim 10^{15} \text{cm}$  and during the period of this stage  $\sim 3 \cdot 10^{15} \text{s}$ , up to  $\sim 10^{-9} S_3^{-1}$  of O-helium atoms per nucleon can be captured [18, 30]. In the Supernova explosion these OHe atoms are disrupted in collisions with particles in the front of shock wave and acceleration of free  $X^{--}$  by regular mechanism gives the corresponding fraction in cosmic rays. However, this picture needs detailed analysis, based on the development of OHe nuclear physics and numerical studies of OHe evolution in the stellar matter.

If these mechanisms of  $X^{--}$  acceleration are effective, the anomalous low  $Z/A$  component of  $-2$  charged  $X^{--}$  can be present in cosmic rays at the level  $X/p \sim n_X/n_g \sim 10^{-9} S_3^{-1}$ , and be within the reach for PAMELA and AMS02 cosmic ray experiments.

In the framework of Walking Technicolor model the excess of both stable  $X^{--}$  and  $Y^{++}$  is possible [18], the latter being two-three orders of magnitude smaller, than the former. It leads to the two-component composite dark matter scenario with the dominant OHe accompanied by a subdominant WIMP-like component of  $(X^{--} Y^{++})$  bound systems. Technibaryons and technileptons can be metastable and decays of  $X^{--}$  and  $Y^{++}$  can provide explanation for anomalies, observed in high energy cosmic positron spectrum by PAMELA and in high energy electron spectrum by FERMI and ATIC.

### Positron annihilation and gamma lines in galactic bulge

Inelastic interaction of O-helium with the matter in the interstellar space and its de-excitation can give rise to radiation in the range from few keV to few MeV. In the galactic bulge with radius  $r_b \sim 1 \text{kpc}$  the number density of O-helium can reach the value  $n_o \approx 3 \cdot 10^{-3} / S_3 \text{cm}^{-3}$  and the collision rate of O-helium in this central region was estimated in [21]:  $dN/dt = n_o^2 \sigma v_h 4\pi r_b^3 / 3 \approx 3 \cdot 10^{42} S_3^{-2} \text{s}^{-1}$ . At the velocity of  $v_h \sim 3 \cdot 10^7 \text{cm/s}$  energy transfer in such collisions is  $\Delta E \sim 1 \text{MeV} S_3$ . These collisions can lead to excitation of O-helium. If 2S level is excited, pair production dominates over two-photon channel in the de-excitation by  $E0$  transition and positron production with the rate  $3 \cdot 10^{42} S_3^{-2} \text{s}^{-1}$  is not accompanied by strong gamma signal. According to [31] this rate of positron production for  $S_3 \sim 1$  is sufficient to explain the excess in positron annihilation line from bulge, measured by INTEGRAL (see [32] for review and references). If OHe levels with nonzero orbital momentum are excited, gamma lines should be observed from transitions ( $n > m$ )  $E_{nm} = 1.598 \text{MeV} (1/m^2 - 1/n^2)$  (or from the similar transitions corresponding to the case  $I_o = 1.287 \text{MeV}$ ) at the level  $3 \cdot 10^{-4} S_3^{-2} (\text{cm}^2 \text{sMeVster})^{-1}$ .

## O-HELIUM IN THE TERRESTRIAL MATTER

The evident consequence of the O-helium dark matter is its inevitable presence in the terrestrial matter, which appears opaque to O-helium and stores all its in-falling flux.

Such neutral ( ${}^4\text{He}^{++} X^{--}$ ) "atoms" may provide a catalysis of cold nuclear reactions in ordinary matter (much more effectively than muon catalysis). This effect needs a special and thorough investigation. On the other hand,  $X^{--}$

capture by nuclei, heavier than helium, can lead to production of anomalous isotopes, but the arguments, presented in [9, 13, 15] indicate that their abundance should be below the experimental upper limits.

It should be noted that the nuclear cross section of the O-helium interaction with matter escapes the severe constraints [23] on strongly interacting dark matter particles (SIMPs) [22, 23] imposed by the XQC experiment [24]. Therefore, a special strategy of direct O-helium search is needed, as it was proposed in [33].

After they fall down terrestrial surface the in-falling *OHe* particles are effectively slowed down due to elastic collisions with matter. Then they drift, sinking down towards the center of the Earth with velocity

$$V = \frac{g}{n\sigma v} \approx 80S_3A^{1/2} \text{ cm/s}. \quad (5)$$

Here  $A \sim 30$  is the average atomic weight in terrestrial surface matter,  $n = 2.4 \cdot 10^{24}/A$  is the number of terrestrial atomic nuclei,  $\sigma v$  is the rate of nuclear collisions and  $g = 980 \text{ cm/s}^2$ .

Near the Earth's surface, the O-helium abundance is determined by the equilibrium between the in-falling and down-drifting fluxes.

The in-falling O-helium flux from dark matter halo is

$$F = \frac{n_0}{8\pi} \cdot |\overline{V}_h + \overline{V}_E|,$$

where  $V_h$ -speed of Solar System (220 km/s),  $V_E$ -speed of Earth (29.5 km/s) and  $n_0 = 3 \cdot 10^{-4} S_3^{-1} \text{ cm}^{-3}$  is the local density of O-helium dark matter. Here, for qualitative estimation, we don't take into account velocity dispersion and distribution of particles in the incoming flux that can lead to significant effect.

At a depth  $L$  below the Earth's surface, the drift timescale is  $t_{dr} \sim L/V$ , where  $V \sim 400S_3 \text{ cm/s}$  is given by Eq. (5). It means that the change of the incoming flux, caused by the motion of the Earth along its orbit, should lead at the depth  $L \sim 10^5 \text{ cm}$  to the corresponding change in the equilibrium underground concentration of *OHe* on the timescale  $t_{dr} \approx 2.5 \cdot 10^2 S_3^{-1} \text{ s}$ .

In underground detectors, *OHe* "atoms" are slowed down to thermal energies and give rise to energy transfer  $\sim 2.5 \cdot 10^{-4} \text{ eVA}/S_3$ , far below the threshold for direct dark matter detection. It makes this form of dark matter insensitive to the severe CDMS [34] and XENON100 constraints [35]. However, *OHe* reactions with the matter of underground detectors can lead to observable effects.

The equilibrium concentration, which is established in the matter of underground detectors, is given by

$$n_{oE} = \frac{2\pi \cdot F}{V} = n_{oE}^{(1)} + n_{oE}^{(2)} \cdot \sin(\omega(t - t_0)), \quad (6)$$

where  $\omega = 2\pi/T$ ,  $T = 1 \text{ yr}$  and  $t_0$  is the phase. The averaged concentration is given by

$$n_{oE}^{(1)} = \frac{n_o}{320S_3A_{med}^{1/2}} V_h \quad (7)$$

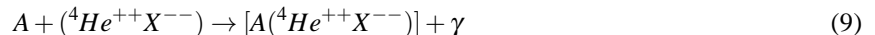
and the annual modulation of concentration is characterized by

$$n_{oE}^{(2)} = \frac{n_o}{640S_3A_{med}^{1/2}} V_E \quad (8)$$

The rate of nuclear reactions of *OHe* with nuclei is proportional to the local concentration and the energy release in these reactions should lead to observable signal. There are two parts of the signal: the one determined by the constant part and annual modulation, which is concerned by the strategy of dark matter search in DAMA experiment [28].

## LOW ENERGY BOUND STATE OF O-HELIUM WITH NUCLEI

Our explanation [19, 20, 26] of the results of DAMA/NaI or DAMA/LIBRA experiments is based on the idea that *OHe*, slowed down in the matter of detector, can form a few keV bound state with nucleus, in which *OHe* is situated **beyond** the nucleus. Therefore the positive result of these experiments is explained by reaction



with nuclei in DAMA detector. In our earlier studies [19, 20, 26] the conditions were found, under which both sodium and iodine nuclei have a few keV bound states with OHe, explaining the results of DAMA experiments by OHe radiative capture to these levels. Here we extend the set of our solutions by the case, when the results of DAMA experiment can be explained by radiative OHe capture by sodium only and there are no such bound states with iodine and Tl.

## Low energy bound state of O-helium with nuclei

Schrodinger equation for OHe-nucleus system is reduced (taking apart the equation for the center of mass) to the equation of relative motion for the reduced mass

$$m = \frac{Am_p m_o}{Am_p + m_o}, \quad (10)$$

where  $m_p$  is the mass of proton and  $m_o \approx M_X + 4m_p$  is the mass of OHe. Since  $m_o \approx M_X \gg Am_p$ , center of mass of Ohe-nucleus system approximately coincides with the position of  $X^{--}$ .

In the case of orbital momentum  $l=0$  the wave functions depend only on  $r$ .

The approach of [19, 20, 26, 36, 37, 38] assumes the following picture: at the distances larger, than its size, OHe is neutral, being only the source of a Coulomb field of  $X^{--}$  screened by *He* shell

$$U_c = \frac{Z_X Z \alpha \cdot F_X(r)}{r}, \quad (11)$$

where  $Z_X = -2$  is the charge of  $X^{--}$ ,  $Z$  is charge of nucleus,  $F_X(r) = (1 + r/r_o) \exp(-2r/r_o)$  is the screening factor of Coulomb potential (see e.g.[39]) of  $X^{--}$  and  $r_o$  is the size of OHe. Owing to the negative sign of  $Z_X = -2$ , this potential provides attraction of nucleus to OHe.

Then helium shell of OHe starts to feel Yukawa exponential tail of attraction of nucleus to *He* due to scalar-isoscalar nuclear potential. It should be noted that scalar-isoscalar nature of He nucleus excludes its nuclear interaction due to  $\pi$  or  $\rho$  meson exchange, so that the main role in its nuclear interaction outside the nucleus plays  $\sigma$  meson exchange, on which nuclear physics data are not very definite. The nuclear potential depends on the relative distance between He and nucleus and we take it in the form

$$U_n = -\frac{A_{He} A g^2 \exp(-\mu|\vec{r} - \vec{\rho}|)}{|\vec{r} - \vec{\rho}|}. \quad (12)$$

Here  $\vec{r}$  is radius vector to nucleus,  $\vec{\rho}$  is the radius vector to He in OHe,  $A_{He} = 4$  is atomic weight of helium,  $A$  is atomic weight of nucleus,  $\mu$  and  $g^2$  are the mass and coupling of  $\sigma$  meson - mediator of nuclear attraction.

Strictly speaking, starting from this point we should deal with a three-body problem for the system of He, nucleus and  $X^{--}$  and the correct quantum mechanical description should be based on the cylindrical and not spherical symmetry. In the present work we use the approximation of spherical symmetry and take into account nuclear attraction beyond the nucleus in a two different ways: 1) nuclear attraction doesn't influence the structure of OHe, so that the Yukawa potential (12) is averaged over  $|\vec{\rho}|$  for spherically symmetric wave function of He shell in OHe; 2) nuclear attraction changes the structure of OHe so that He takes the position  $|\vec{\rho}| = r_o$ , which is most close to the nucleus. Due to strong attraction of He by the nucleus the second case (which is labeled "b" in successive numerical calculations) seems more probable. In the lack of the exact solution of the problem we present both the results, corresponding to the first case (which are labeled "m" in successive numerical calculations), and to the second case (which is labeled "b") in order to demonstrate high sensitivity of the numerical results to choice of parameters.

In the both cases nuclear attraction results in the polarization of OHe and the mutual attraction of nucleus and OHe is changed by Coulomb repulsion of *He* shell. Taking into account Coulomb attraction of nucleus by  $X^{--}$  one obtains dipole Coulomb barrier of the form

$$U_d = \frac{Z_{He} Z \alpha r_o}{r^2}. \quad (13)$$

When helium is completely merged with the nucleus the interaction is reduced to the oscillatory potential (14) of  $X^{--}$  with homogeneously charged merged nucleus with the charge  $Z + 2$ , given by

$$E_m = \frac{3}{2} \left( \frac{(Z+2)Z\alpha}{R} - \frac{1}{R} \left( \frac{(Z+2)Z\alpha}{(A+4)m_p R} \right)^{1/2} \right). \quad (14)$$

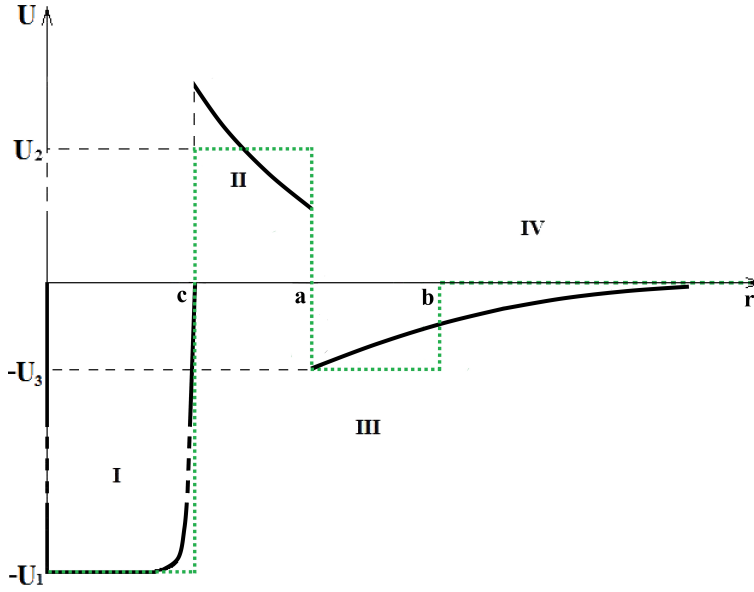


**FIGURE 1.** The approximation of rectangular well for potential of OHe-nucleus system.

To simplify the solution of Schroedinger equation we approximate the potentials (11)-(14) by a rectangular potential that consists of a potential well with the depth  $U_1$  at  $r < c = R$ , where  $R$  is the radius of nucleus, of a rectangular dipole Coulomb potential barrier  $U_2$  at  $R \leq r < a = R + r_o + r_{he}$ , where  $r_{he}$  is radius of helium nucleus, and of the outer potential well  $U_3$ , formed by the Yukawa nuclear interaction (12) and residual Coulomb interaction (11). The values of  $U_1$  and  $U_2$  were obtained by the averaging of the (14) and (13) in the corresponding regions, while  $U_3$  was equal to the value of the nuclear potential (12) at  $r = a$  and the width of this outer rectangular well (position of the point b) was obtained by the integral of the sum of potentials (12) and (11) from  $a$  to  $\infty$ . It leads to the approximate potential, presented on Fig. 1.

Solutions of Schroedinger equation for each of the four regions, indicated on Fig. 1, are given in textbooks (see e.g.[39]) and their sewing determines the condition, under which a low-energy OHe-nucleus bound state appears in the region III.

The energy of this bound state and its existence strongly depend on the parameters  $\mu$  and  $g^2$  of nuclear potential (12). On the Fig. 2 the regions of these parameters, giving 4 keV energy level in OHe bound state with sodium are presented. Radiative capture to this level can explain results of DAMA/NaI and DAMA/LIBRA experiments with the account for their energy resolution [40]. The lower shaded region on Fig. 2 corresponds to the case of nuclear Yukawa potential  $U_{3m}$ , averaged over the orbit of He in OHe, while the upper region corresponds to the case of nuclear Yukawa potential  $U_{3b}$  with the position of He most close to the nucleus at  $\rho = r_o$ . The result is also sensitive to the precise value of  $d_o$ , which determines the size of nuclei  $R = d_o A^{1/3}$ . The two narrow strips in each region correspond to the experimentally most probable value  $d_o = 1.2/(200 \text{ MeV})$ . In these calculations the mass of OHe was taken equal to  $m_o = 1 \text{ TeV}$ , however the results weakly depend on the value of  $m_o > 1 \text{ TeV}$ .

It is interesting that the values of  $\mu$  on Fig. 2 are compatible with the results of recent experimental measurements of mass of sigma meson ( $\mu \sim 404 \text{ MeV}$ ) [41].

The rate of radiative capture of OHe by nuclei can be calculated [19, 20] with the use of the analogy with the radiative capture of neutron by proton with the account for: i) absence of M1 transition that follows from conservation of orbital momentum and ii) suppression of E1 transition in the case of OHe. Since OHe is isoscalar, isovector E1 transition can take place in OHe-nucleus system only due to effect of isospin nonconservation, which can be measured by the factor  $f = (m_n - m_p)/m_N \approx 1.4 \cdot 10^{-3}$ , corresponding to the difference of mass of neutron,  $m_n$ , and proton,  $m_p$ , relative to the mass of nucleon,  $m_N$ . In the result the rate of OHe radiative capture by nucleus with atomic number  $A$  and charge  $Z$  to the energy level  $E$  in the medium with temperature  $T$  is given by

$$\sigma_v = \frac{f\pi\alpha}{m_p^2} \frac{3}{\sqrt{2}} \left(\frac{Z}{A}\right)^2 \frac{T}{\sqrt{Am_p E}}. \quad (15)$$

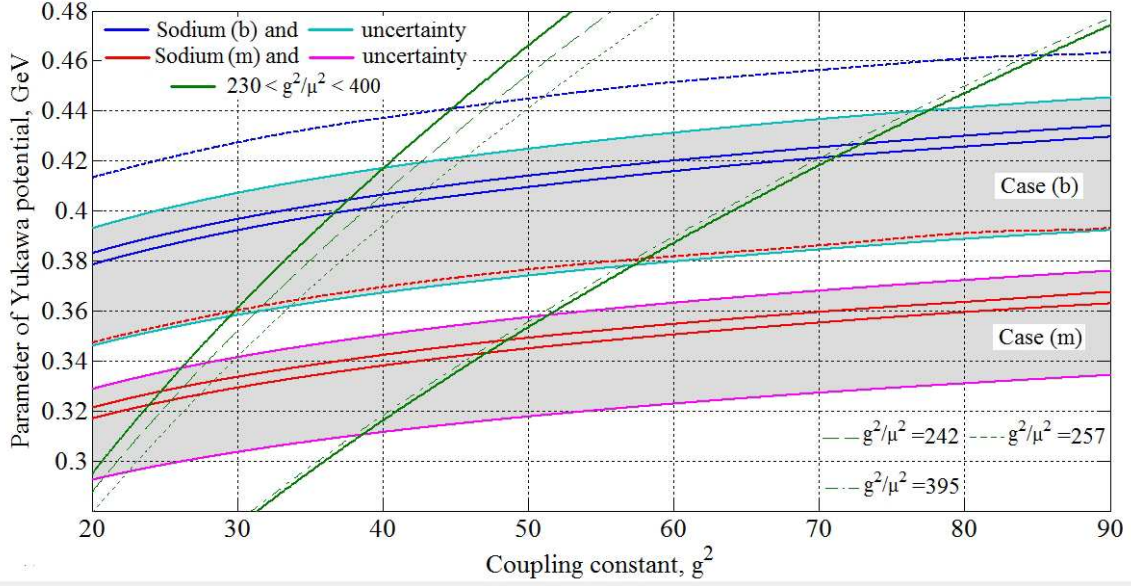


**FIGURE 2.** The region of parameters  $\mu$  and  $g^2$ , for which Na-OHe system has a level in the interval 4 keV. Two lines determine at  $d_o = 1.2/(200\text{MeV})$  the region of parameters, at which the bound system of this element with OHe has a 4 keV level. In the region between the two strips the energy of level is below 4 keV. There are also indicated the range of  $g^2/\mu^2$  (dashed lines) as well as their preferred values (thin lines) determined in [42] from parametrization of the relativistic  $(\sigma - \omega)$  model for nuclear matter. The uncertainty in the determination of parameter  $1.15/(200\text{MeV}) < d_o < 1.3/(200\text{MeV})$  results in the uncertainty of  $\mu$  and  $g^2$  shown by the shaded regions surrounding the lines. The case of nuclear Yukawa potential  $U_{3m}$ , averaged over the orbit of He in OHe, corresponds to the lower lines and shaded region, while the upper lines and shaded region around them illustrate the case of nuclear Yukawa potential  $U_{3b}$  with the position of He most close to the nucleus at  $\rho = r_o$ .

Formation of OHe-nucleus bound system leads to energy release of its binding energy, detected as ionization signal. In the context of our approach the existence of annual modulations of this signal in the range 2-6 keV and absence of such effect at energies above 6 keV means that binding energy of Na-OHe system in DAMA experiment should not exceed 6 keV, being in the range 2-4 keV. The amplitude of annual modulation of ionization signal (measured in counts per day per kg, cpd/kg) is given by

$$\zeta = \frac{3\pi\alpha \cdot n_o N_A V_E t Q}{640\sqrt{2} A_{med}^{1/2} (A_i + A_{Na})} \frac{f}{S_3 m_p^2} \left(\frac{Z_i}{A_i}\right)^2 \frac{T}{\sqrt{A_i m_p E_i}} = a_i \frac{f}{S_3^2} \left(\frac{Z_i}{A_i}\right)^2 \frac{T}{\sqrt{A_i m_p E_i}}. \quad (16)$$

Here  $N_A$  is Avogadro number,  $i$  denotes Na, for which numerical factor  $a_i = 4.3 \cdot 10^{10}$ ,  $Q = 10^3$  (corresponding to 1kg of the matter of detector),  $t = 86400\text{s}$ ,  $E_i$  is the binding energy of Na-OHe system and  $n_o = 3 \cdot 10^{-4} \text{S}_3^{-1} \text{cm}^{-3}$  is the local density of O-helium dark matter near the Earth. The value of  $\zeta$  should be compared with the integrated over energy bins signals in DAMA/NaI and DAMA/LIBRA experiments and the result of these experiments can be reproduced for  $E_{Na} = 3\text{keV}$ . The account for energy resolution in DAMA experiments [40] can explain the observed energy distribution of the signal from monochromatic photon (with  $E_{Na} = 3\text{keV}$ ) emitted in OHe radiative capture.

At the corresponding values of  $\mu$  and  $g^2$  there is no binding of OHe with iodine and thallium.

It should be noted that the results of DAMA experiment exhibit also absence of annual modulations at the energy of MeV-tens MeV. Energy release in this range should take place, if OHe-nucleus system comes to the deep level inside the nucleus (in the region I of Fig. 1). This transition implies tunneling through dipole Coulomb barrier and is suppressed below the experimental limits.

## OHe radiative capture by other nuclei

The important qualitative feature of the presented solution is the restricted range of intermediate nuclei, in which the OHe-nucleus state beyond nuclei is possible. For the chosen range of nuclear parameters, reproducing the results of



**TABLE 1.** Effects of OHe in pure silicon cryogenic detector in the case m for nuclear Yukawa potential  $U_{3m}$ , averaged over the orbit of He in OHe [37].

$g^2/\mu^2, GeV^{-1}$	242	242	257	257	395	395
Energy, keV	2.7	31.9	3.0	33.2	6.1	41.9
$\sigma V \cdot 10^{-33}, cm^3/s$	19.3	5.6	18.3	5.5	12.8	4.9
$\xi \cdot 10^{-2}, cpd/kg$	10.8	3.1	10.2	3.1	7.2	2.7

**TABLE 2.** Effects of OHe in pure silicon cryogenic detector for the case of the nuclear Yukawa potential  $U_{3b}$  with the position of He most close to the nucleus [37].

$g^2/\mu^2, GeV^{-1}$	242	242	257	257	395	395
Energy, keV	29.8	89.7	31.2	92.0	42.0	110.0
$\sigma V \cdot 10^{-33}, cm^3/s$	5.8	3.3	5.7	3.3	4.9	3.0
$\xi \cdot 10^{-2}, cpd/kg$	3.3	1.9	3.2	1.9	2.7	1.7

DAMA/NaI and DAMA/LIBRA, we can calculate the binding energy of OHe-nucleus states in nuclei, corresponding to chemical composition of set-ups in other experiments. It turns out that there are no such states for light and heavy nuclei. In the case of nuclear Yukawa potential  $U_{3b}$ , corresponding to the position of He most close to the nucleus at  $\rho = r_o$ , the range of nuclei with bound states with OHe corresponds to the part of periodic table between B and Ti. This result is stable independent on the used scheme of numerical calculations. In the case of potential  $U_{3m}$ , averaged over the orbit of He in OHe, there are no OHe bound states with nuclei, lighter than Be and heavier than Ti. However, the results are very sensitive to the numerical factors of calculations and the existence of OHe-Ge and OHe-Ga bound states at a narrow window of parameters  $\mu$  and  $g^2$  turns to be strongly dependent on these factors so that change in numbers smaller than 1% can give qualitatively different result for Ge and Ga. Both for the cases (b) and (m) there is a stable conclusion that there are no OHe-nucleus bound states with Xe, I and Tl.

For the experimentally preferred value  $d_o = 1.2/(200\text{MeV})$  the results of calculation of the binding energy of OHe-nucleus systems for carbon, oxygen, fluorine, argon, silicon, aluminium and chlorine are presented on Fig. 3 for the case of the nuclear Yukawa potential  $U_{3b}$  (upper figure) and  $U_{3m}$  (lower figure). The difference in these results demonstrates their high sensitivity to the choice of parameters. For the parameters, reproducing results of DAMA experiment the predicted energy level of OHe-silicon bound state is generally beyond the range 2-6 keV, being in the most cases in the range of 30-40 keV or 90-110 keV by absolute value. It makes elusive a possibility to test DAMA results by search for ionization signal in the same range 2-6 keV in other set-ups with content that differs from Na and I. Even in the extreme case (m) of ionization signal in the range 2-6 keV our approach naturally predicts its suppression in accordance with the results of CDMS [43].

It should be noted that strong sensitivity of the existence of the OHe-Ge bound state to the values of numerical factors [37] doesn't exclude such state for some window of nuclear physics parameters. The corresponding binding energy would be about 450-460 keV, what proves the above statement even in that case.

Since OHe capture rate is proportional to the temperature, it looks like it is suppressed in cryogenic detectors by a factor of order  $10^{-4}$ . However, for the size of cryogenic devices less, than few tens meters, OHe gas in them has the thermal velocity of the surrounding matter and the suppression relative to room temperature is only  $\sim m_A/m_o$ . Then the rate of OHe radiative capture in cryogenic detectors is given by Eq.(15), in which room temperature  $T$  is multiplied by factor  $m_A/m_o$ , and the ionization signal (measured in counts per day per kg, cpd/kg) is given by Eq.(16) with the same correction for  $T$  supplemented by additional factors  $2V_h/V_E$  and  $(A_I + A_{Na})/A_i$ , where  $i$  denotes Si. To illustrate possible effects of OHe in various cryogenic detectors we give in Tables 1 and 2 energy release, radiative capture rate and counts per day per kg for the pure silicon for the preferred values of nuclear parameters.

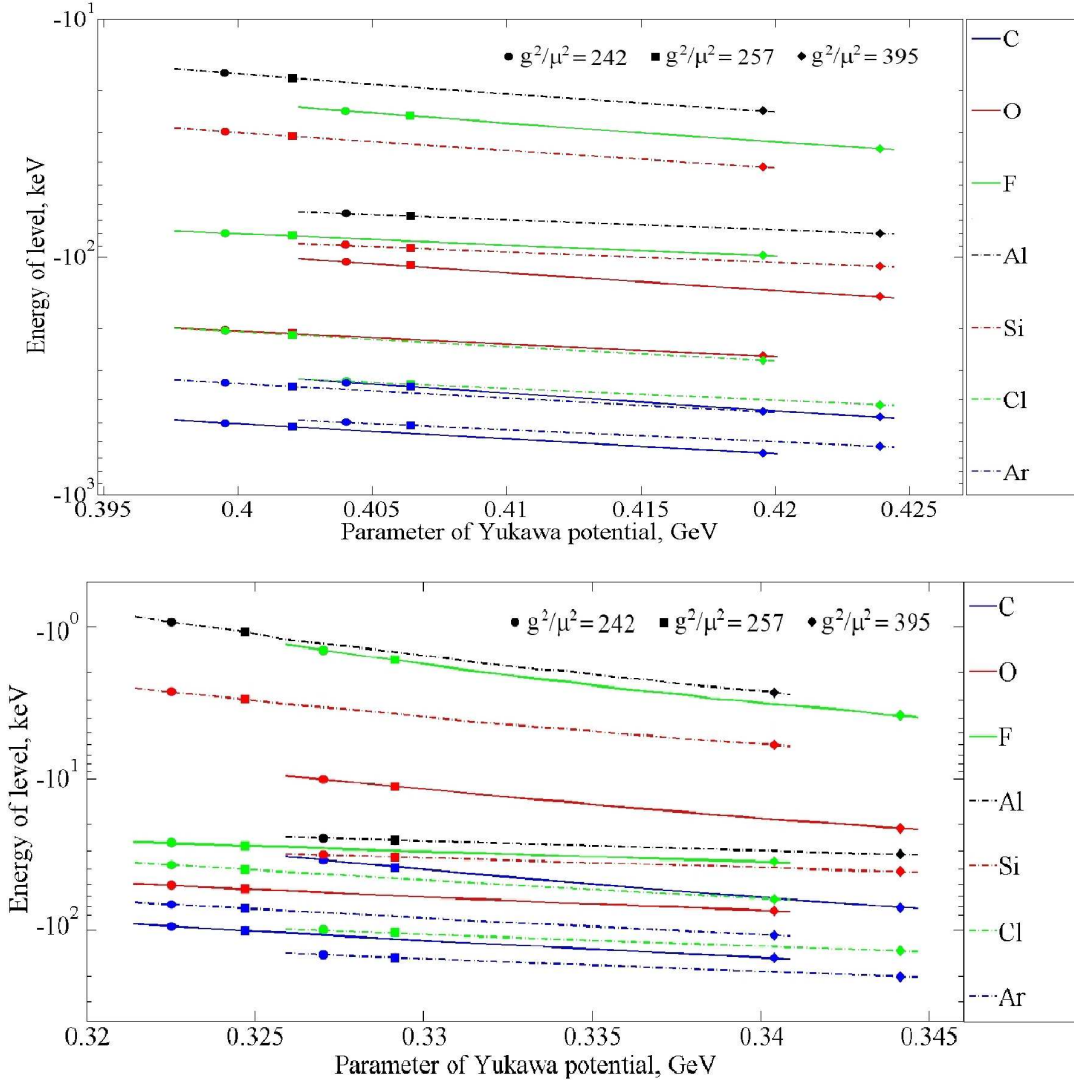


**FIGURE 3.** Energy levels in OHe bound system with carbon, oxygen, fluorine, argon, silicon, aluminium and chlorine for the case of the nuclear Yukawa potential  $U_{3b}$  (upper figure) and  $U_{3m}$  (lower figure). The predictions are given for the range of  $g^2/\mu^2$  determined in [42] from parametrization of the relativistic ( $\sigma - \omega$ ) model for nuclear matter. The preferred values of  $g^2/\mu^2$  are indicated by the corresponding marks (squares or circles).

## CONCLUSIONS

To be present in the modern Universe, dark matter should survive to the present time. It assumes a conservation law for dark matter particles, what implies these particles to possess some new fundamental symmetry and corresponding conserved charge. If particles possess new gauge U(1) symmetry, they can bind by the corresponding Coulomb-like interaction in dark atoms, emitting dark U(1) photons. Here, we have studied a possibility that dark matter particles possess ordinary electric charge and are bound in dark atoms by ordinary Coulomb interaction. However restricted, this possibility is not excluded by observations. The existence of heavy stable charged particles may not only be compatible with the experimental constraints but can even lead to composite dark matter scenario of nuclear interacting Warmer than Cold Dark Matter. This new form of dark matter can provide explanation of excess of positron annihilation line radiation, observed by INTEGRAL in the galactic bulge.

In the first three minutes primordial stable particles with charge -2 are bound with helium so that their specific features are shielded by a nuclear interacting helium shell that determines their successive evolution in the form of dark OHe atoms. Detailed analysis of this evolution implies development of OHe nuclear physics that is now under way. Its first results indicate that OHe experiences dominantly elastic collisions with the matter and that its inelastic collisions with capture inside nuclei are strongly suppressed. It provides qualitative proof of earlier guess that formation of anomalous isotopes due to OHe capture is within the experimental upper limits.

Destruction of OHe, e.g. by cosmic rays or in SN explosions gives rise to free  $X^{--}$ , but relative amount of such free X as compared with those bound in OHe is at least by factor  $10^7$  smaller in the Galaxy and their penetration in the Solar System is hindered by the Solar wind. We qualitatively expect existence of an X component of cosmic rays, but of course we need more studies to check other possible signatures of free X. The search for stable -2 charge component of cosmic rays is challenging for PAMELA and AMS02 experiments. Decays of heavy charged constituents of composite dark matter can provide explanation for anomalies in spectra of cosmic high energy positrons and electrons, observed by PAMELA, FERMI and ATIC.

In the surrounding terrestrial matter OHe concentration is regulated by the equilibrium between the down streaming diffusion to the center of the Earth and the incoming cosmic flux. As it follows from Eq. (7) this averaged equilibrium concentration is of the order of few species per  $\text{cm}^3$ . Effects of these species in the matter need, certainly, special studies but in the first approximation it seems that OHe signatures in the underground experiments, discussed in the present paper, provide their most sensitive probe.

In the context of our approach search for heavy stable charged quarks and leptons at LHC acquires the significance of experimental probe for components of cosmological composite dark matter. Accelerator test for composite  $X^{--}$  can be only indirect: in the lack of possibility of direct search for triple heavy quark or antiquark states it is possible to search for heavy hadrons, composed of single  $U$  or  $\bar{U}$  and light quarks. One can analyze mass spectrum of these hadrons and find the correlations, by which they can be in principle detected and discriminated from other similar particles, like R-hadrons.

The way to search for AC leptons and techniparticles looks much more straightforward. The set of experimental signatures for these particles can provide their clear distinction from other hypothetical exotic particles.

The results of dark matter search in experiments DAMA/NaI and DAMA/LIBRA can be explained in the framework of our scenario without contradiction with the results of other groups. This scenario can be realized in different frameworks, in particular, in the extensions of Standard Model, based on the approach of almost commutative geometry, in the model of stable quarks of 4th generation that can be naturally embedded in the heterotic superstring phenomenology, in the models of stable technileptons and/or techniquarks, following from Minimal Walking Technicolor model or in the approach unifying spin and charges. Our approach contains distinct features, by which the present explanation can be distinguished from other recent approaches to this problem [44] (see also for review and more references in [45]).

The proposed explanation is based on the mechanism of low energy binding of OHe with nuclei. Within the uncertainty of nuclear physics parameters there exists a range at which OHe binding energy with sodium is in the interval 2-4 keV. Radiative capture of OHe to this bound state leads to the corresponding energy release observed as an ionization signal in DAMA detector.

OHe concentration in the matter of underground detectors is determined by the equilibrium between the incoming cosmic flux of OHe and diffusion towards the center of Earth. It is rapidly adjusted and follows the change in this flux with the relaxation time of few minutes. Therefore the rate of radiative capture of OHe should experience annual modulations reflected in annual modulations of the ionization signal from these reactions.

An inevitable consequence of the proposed explanation is appearance in the matter of DAMA/NaI or DAMA/LIBRA detector anomalous superheavy isotopes of sodium, having the mass roughly by  $m_o$  larger, than ordinary isotopes of these elements. If the atoms of these anomalous isotopes are not completely ionized, their mobility is determined by atomic cross sections and becomes about 9 orders of magnitude smaller, than for O-helium. It provides their conservation in the matter of detector. Therefore mass-spectroscopic analysis of this matter can provide additional test for the O-helium nature of DAMA signal. Methods of such analysis should take into account the fragile nature of OHe-Na bound states, since their binding energy is only few keV.

With the account for high sensitivity of the numerical results to the values of nuclear parameters and for the approximations, made in the calculations, the presented results can be considered only as an illustration of the possibility to explain puzzles of dark matter search in the framework of composite dark matter scenario. An interesting feature of this explanation is a conclusion that the ionization signal expected in detectors with the content, different from NaI, can be dominantly in the energy range beyond 2-6 keV. Moreover, it can be absent in detectors, containing heavy nuclei (e.g. xenon). Therefore test of results of DAMA/NaI and DAMA/LIBRA experiments by other experimental

groups can become a very nontrivial task.

Our results show that the ionization signal, detected by DAMA, may be absent in detectors containing light elements. In particular, there is predicted no low-energy binding of OHe with  ${}^3\text{He}$  and correspondingly no ionization signal in keV range in the designed  ${}^3\text{He}$  dark matter detectors. Therefore development of experimental methods of dark matter detection will extend the possibilities to test hypothesis of composite dark matter.

It is interesting to note that in the framework of our approach positive result of experimental search for WIMPs by effect of their nuclear recoil would be a signature for a multicomponent nature of dark matter. Such OHe+WIMPs multicomponent dark matter scenarios naturally follow from AC model [13] and can be realized in models of Walking technicolor [18].

The presented approach sheds new light on the physical nature of dark matter. Specific properties of composite dark matter and its constituents are challenging for their experimental search. OHe interaction with matter is an important aspect of these studies. In this context positive result of DAMA/NaI and DAMA/LIBRA experiments may be a signature for exciting phenomena of O-helium nuclear physics.

## ACKNOWLEDGMENTS

We express our gratitude to Jonathan J. Dickau for kind invitation to contribute this issue of Prespacetime Journal focusing on Cosmology and Gravity.

## REFERENCES

1. M.Yu. Khlopov *Cosmoparticle physics* (World Scientific, Singapore, 1999).
2. M.Yu. Khlopov in *Cosmion-94*, Eds. M.Yu.Khlopov et al. (Editions frontieres, 1996) P. 67; M. Y. Khlopov in hep-ph/0612250, p 51.
3. M. Y. Khlopov, *Bled Workshops in Physics* **8**, 114 (2007); in arXiv:0711.4681, p. 114; M. Y. Khlopov and N. S. Mankoč-Borštnik, *ibid*, p. 195.
4. A. G. Polnarev and M. Y. Khlopov, *Sov. Phys. Usp.* **28**, 213 (1985) [*Usp. Fiz. Nauk* **145**, 369 (1985)]; M. Y. Khlopov, *Res. Astron. Astrophys.* **10**, 495 (2010) [arXiv:0801.0116 [astro-ph]].
5. D. C. Dai, K. Freese and D. Stojkovic, *JCAP* **0906** (2009) 023 [arXiv:0904.3331 [hep-ph]].
6. S. L. Glashow, arXiv:hep-ph/0504287.
7. D. Fargion and M. Khlopov, arXiv:hep-ph/0507087.
8. K.M.Belotsky *et al*, *Gravitation and Cosmology* **11**, 3 (2005)
9. M.Yu. Khlopov, *JETP Lett.* **83**, 1 (2006).
10. K. Belotsky *et al*, arXiv:astro-ph/0602261. K. Belotsky *et al*, *Gravitation and Cosmology* **12**, 1 (2006); K. Belotsky *et al*, arXiv:0806.1067 [astro-ph].
11. M. Y. Khlopov, arXiv:astro-ph/0607048.
12. C. A. Stephan, arXiv:hep-th/0509213.
13. D. Fargion *et al*, *Class. Quantum Grav.* **23**, 7305 (2006); M. Y. Khlopov and C. A. Stephan, arXiv:astro-ph/0603187.
14. A. Connes *Noncommutative Geometry* (Academic Press, London and San Diego, 1994).
15. M. Y. Khlopov and C. Kouvaris, *Phys. Rev. D* **77**, 065002 (2008).
16. F. Sannino and K. Tuominen, *Phys. Rev. D* **71**, 051901 (2005); D. K. Hong *et al*, *Phys. Lett. B* **597**, 89 (2004); D. D. Dietrich *et al*, *Phys. Rev. D* **72**, 055001 (2005); D. D. Dietrich *et al*, arXiv:hep-ph/0510217; S. B. Gudnason *et al*, *Phys. Rev. D* **73**, 115003 (2006); S. B. Gudnason *et al*, *Phys. Rev. D* **74**, 095008 (2006).
17. N.S. Mankoč Borštnik, This Volume; A. Borštnik Bračič, N.S. Mankoč Borštnik, *Phys. Rev. D* **74**, 073013 (2006); N.S. Mankoč Borštnik, *Mod. Phys. Lett. A* **10**, 587 (1995); N.S. Mankoč Borštnik, *Int. J. Theor. Phys.* **40**, 315 (2001); G. Bregar, M. Breskvar, D. Lukman, N.S. Mankoč Borštnik, *New J. of Phys.* **10**, 093002 (2008).
18. M. Y. Khlopov and C. Kouvaris, *Phys. Rev. D* **78**, 065040 (2008)
19. M. Y. Khlopov, *AIP Conf. Proc.* **1241** (2010) 388 [arXiv:0911.5685 [astro-ph.CO]].
20. M. Y. Khlopov, A. G. Mayorov and E. Y. Soldatov, *Int. J. Mod. Phys. D* **19** (2010) 1385 [arXiv:1003.1144 [astro-ph.CO]].
21. M. Y. Khlopov, arXiv:0806.3581 [astro-ph].
22. C. B. Dover *et al*, *Phys. Rev. Lett.* **42**, 1117 (1979); S. Wolfram, *Phys. Lett. B* **82**, 65 (1979); G. D. Starkman *et al*, *Phys. Rev. D* **41**, 3594 (1990); D. Javorsek *et al*, *Phys. Rev. Lett.* **87**, 231804 (2001); S. Mitra, *Phys. Rev. D* **70**, 103517 (2004); G. D. Mack *et al*, *Phys. Rev. D* **76**, 043523 (2007);
23. B. D. Wandelt *et al*, arXiv:astro-ph/0006344; P. C. McGuire and P. J. Steinhardt, arXiv:astro-ph/0105567; G. Zaharijas and G. R. Farrar, *Phys. Rev. D* **72**, 083502 (2005)
24. D. McCammon *et al*, *Nucl. Instrum. Methods A* **370**, 266 (1996); D. McCammon *et al*, *Astrophys. J.* **576**, 188 (2002).
25. M. Y. Khlopov, arXiv:0801.0167 [astro-ph]; M. Y. Khlopov, arXiv:0801.0169 [astro-ph].
26. M. Yu. Khlopov, A. G. Mayorov, E. Yu. Soldatov, *Bled Workshops in Physics* **10**, 79 (2009); arXiv:0911.5606.

27. R. Bernabei *et al.*, *Rivista Nuovo Cimento* **26**, 1 (2003)
28. R. Bernabei *et al.* [DAMA Collaboration], *Eur. Phys. J. C* **56** (2008) 333 [arXiv:0804.2741 [astro-ph]]; R. Bernabei *et al.*, *Eur. Phys. J. C* **67** (2010) 39 [arXiv:1002.1028 [astro-ph.GA]]; R. Bernabei *et al.*, arXiv:1007.0595 [astro-ph.CO].
29. R. N. Cahn and S. L. Glashow, *Science* **213**, 607 (1981); M. Pospelov, *Phys. Rev. Lett.* **98**, 231301 (2007); K. Kohri and F. Takayama, *Phys. Rev. D* **76**, 063507 (2007).
30. K.M.Belotsky, A.G.Mayorov, M.Yu.Khlopov. Charged particles of dark matter in cosmic rays. ISBN 978-5-7262-1280-7, Scientific Session NRNU MEPhI-2010, V.4, P.127
31. D. P. Finkbeiner and N. Weiner, *Phys. Rev. D* **76**, 083519 (2007)
32. B. J. Teegarden *et al.*, *Astrophys. J.* **621**, 296 (2005)
33. K. Belotsky *et al.*, arXiv:astro-ph/0606350.
34. D. S. Akerib *et al.* [CDMS Collaboration], *Phys. Rev. Lett.* **96**, 011302 (2006); Z. Ahmed *et al.* [CDMS Collaboration], arXiv:0802.3530 [astro-ph].
35. E. Aprile *et al.* [XENON100 Collaboration], *Phys. Rev. Lett.* **105** (2010) 131302 [arXiv:1005.0380 [astro-ph.CO]].
36. M. Yu. Khlopov, A. G. Mayorov, E.Yu. Soldatov, *Bled Workshops in Physics* **9**, 24 (2008)
37. M. Y. Khlopov, A. G. Mayorov and E. Y. Soldatov, arXiv:1011.4586
38. M. Y. Khlopov, A. G. Mayorov and E. Y. Soldatov, arXiv:1011.4587
39. L. D. Landau, E. M. Lifshitz *Quantum Mechanics: Non-Relativistic Theory* (Fizmatlit, Moscow, 2004).
40. R. Bernabei *et al.* [DAMA Collaboration], *Nucl. Instrum. Meth. A* **592** (2008) 297 [arXiv:0804.2738 [astro-ph]].
41. Yu. A. Troyan, A. V. Beljaev, A. Y. Troyan, E. B. Plekhanov, A. P. Jerusalemov and S. G. Arakelian, arXiv:1011.3124 [hep-ex].
42. A. b. A. Dadi, *Phys. Rev. C* **82** (2010) 025203 [arXiv:1005.2030 [nucl-th]].
43. O. Kamaev for the CDMS Collaboration, arXiv:0910.3005 [hep-ex].
44. F. Petriello and K. M. Zurek, *JHEP* **0809**, 047 (2008); R. Foot, *Phys. Rev. D* **78**, 043529 (2008); J. L. Feng, J. Kumar and L. E. Strigari, arXiv:0806.3746 [hep-ph]; J. L. Feng, J. Kumar, J. Learned and L. E. Strigari, arXiv:0808.4151 [hep-ph]; E. M. Drobyshevski, arXiv:0811.0151 [astro-ph]; B. Feldstein, A. L. Fitzpatrick and E. Katz, *JCAP* **1001** (2010) 020 [arXiv:0908.2991 [hep-ph]]; Y. Bai and P. J. Fox, *JHEP* **0911** (2009) 052 [arXiv:0909.2900 [hep-ph]]; B. Feldstein, A. L. Fitzpatrick, E. Katz and B. Tweedie, *JCAP* **1003** (2010) 029 [arXiv:0910.0007 [hep-ph]]; A. L. Fitzpatrick, D. Hooper and K. M. Zurek, *Phys. Rev. D* **81** (2010) 115005 [arXiv:1003.0014 [hep-ph]]; S. Andreas, C. Arina, T. Hambye, F. S. Ling and M. H. G. Tytgat, *Phys. Rev. D* **82** (2010) 043522 [arXiv:1003.2595 [hep-ph]]; D. S. M. Alves, S. R. Behbahani, P. Schuster and J. G. Wacker, *JHEP* **1006** (2010) 113 [arXiv:1003.4729 [hep-ph]]; V. Barger, M. McCaskey and G. Shaughnessy, *Phys. Rev. D* **82** (2010) 035019 [arXiv:1005.3328 [hep-ph]]; C. Savage, G. Gelmini, P. Gondolo and K. Freese, arXiv:1006.0972 [astro-ph.CO]; D. Hooper, J. I. Collar, J. Hall and D. McKinsey, arXiv:1007.1005 [hep-ph]; S. Chang, R. F. Lang and N. Weiner, arXiv:1007.2688 [hep-ph]; S. Chang, N. Weiner and I. Yavin, arXiv:1007.4200 [hep-ph]; V. Barger, W. Y. Keung and D. Marfatia, arXiv:1007.4345 [hep-ph]. A. L. Fitzpatrick and K. M. Zurek, arXiv:1007.5325 [hep-ph]; T. Banks, J. F. Fortin and S. Thomas, arXiv:1007.5515 [hep-ph]; B. Feldstein, P. W. Graham and S. Rajendran, arXiv:1008.1988 [hep-ph].
45. G. B. Gelmini, *Int. J. Mod. Phys. A* **23** (2008) 4273 [arXiv:0810.3733 [hep-ph]]; E. Aprile, S. Profumo, *New J. Phys.* **11** (2009) 105002. J. L. Feng, arXiv:1003.0904 [astro-ph.CO].